

# POSSIBLE EVIDENCE OF EARTHQUAKE PRECURSORS OBSERVED IN IONOSPHERIC SCINTILLATION EVENTS OBSERVED FROM SPACEBORNE GNSS-R DATA

C. Molina<sup>1,2</sup>, B.E. Boudriki Semlali<sup>1,2</sup>, H. Park<sup>1,2</sup>, and A. Camps<sup>1,2</sup>

<sup>1</sup>CommSensLab – UPC, Universitat Politècnica de Catalunya – BarcelonaTech

<sup>2</sup>Institute of Space Studies of Catalonia (IEEC) – CTE-UPC

## ABSTRACT

Several factors may induce perturbations on the ionospheric plasma, changing its average electron density and creating small-scale irregularities, changing its shape and altitude. Solar irradiance and space weather are some of the main factors affecting the ionosphere. They produce a seasonal and daily dependence, modulated by the solar cycle, with more ionospheric activity during periods of higher solar activity. Recent studies shows that another source of perturbations for the ionosphere may be related to internal Earth parameters as seismic activity, in particular, earthquakes. In the period before an earthquake, rocks in the lithosphere are subjected to pressures and movements that may create variations of electromagnetic fields and low frequency waves interacting with the ionosphere. In this work, the ionospheric scintillation intensity index or  $S_4$  is estimated from GNSS-R data collected by NASA CYGNSS, and it is correlated with earthquakes events in 2020. Furthermore, it is compared with plasma fluctuation indices measured by ESA Swarm satellites. Two earthquakes in 2020 with magnitudes larger than 7 in the central America region are shown in this work.

**Index Terms**— Ionosphere, earthquake precursor, Swarm, CYGNSS, GNSS-R.

## 1. INTRODUCTION

Ionospheric scintillation is one of the main concerns for satellite communications, GNSS, and Earth Observation (EO) systems. It consists of rapid intensity and phase fluctuations of the electromagnetic waves passing through it. It is known to be driven by solar activity, such as the radiation intensity, varying from day to night; latitude, affecting the incidence angle, and solar cycle phase, which influence the upper atmospheric layers.

Another source of perturbation for the ionosphere comes from the lithosphere and changes in the geomagnetic field. The purpose of this study is to analyze the potential correlations between the ionospheric activity and the internal Earth activity produced by seismic events, i.e. earthquakes.

Even there is a strong consensus on the impossibility to predict Earthquakes, some studies report lithosphere-ionosphere influences exhibited, for example, by magnetic

field variations during aurora periods that correlate to seismic activity [1, 2]. Lithosphere rocks suffer from large pressures in regions where tectonic plates collide or slide with others. This pressure can create electric currents and fields due to the piezoelectric effect, and those electric fields can generate ELF (Extremely Low Frequency) electromagnetic waves that can affect the shape and density of the ionosphere [3].

## 2. DATA SOURCES AND METHOD

In this study, ionospheric anomalies and geomagnetic fields are analyzed to make a correlation with earthquakes. A novel technique introduced in [4] is used to derive the  $S_4$  scintillation indicator from GNSS-R data by measuring the fluctuations in the Signal-to-Noise Ratio of the Delay-Doppler Map (DDM) in reflections over calm water surfaces, following the methodology explained in [5]. GNSS-R data is obtained from NASA Cyclone Global Navigation Satellite System (CYGNSS) mission, a constellation of 8 satellites with an orbital inclination of 35°, covering latitudes from 40°S to 40°N.

To study the global  $S_4$  evolution and anomalies, daily maps have been created by averaging the  $S_4$  samples over oceans within a grid of 1° latitude/longitude bins. The number of samples per bin, and per day varies from around 100 in equatorial regions to 200 at around 30° North and South.

The United States Geological Survey (USGS) database, containing earthquakes magnitude, date, coordinates and depth of the hypocenter is also used. Selecting only the ones with magnitudes larger than 4.5 magnitude there are around 5200 earthquakes in latitudes from 40°S to 40°N, which may be suitable to correlate using CYGNSS data. It is expected that the larger the earthquake magnitude, the larger the ionospheric perturbation produced. During 2020, and within the  $\pm 40^\circ$  latitude range, there were only 96 earthquakes with magnitudes of 6 or larger, and 5 with magnitudes larger or equal than 7.

A set of daily  $S_4$  maps for one year (from October 2019 to October 2020) has been generated. To detect seasonal and geographic anomalies from the typical values, for each pixel in the map, we subtracted the 7-day average following day D from the the preceding 90-day average, according to the

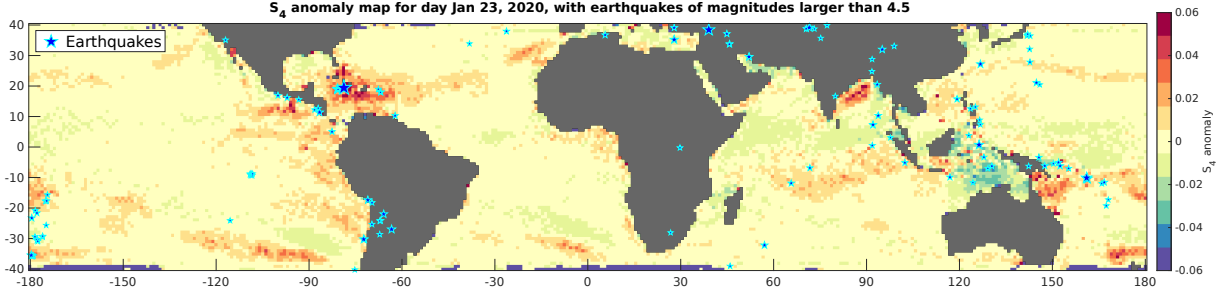


**Fig. 1:**  $S_4$  anomaly map computed from the 7 days following Jan 23, 2020, after subtracting the preceding 90-days average for all oceanic regions between 40°S to 40°N latitude. Blue stars are the earthquake’s epicenters happening in the next 7 days.

expression (1),

$$S_4^*(y, x) = \frac{1}{7} \sum_{d=D}^{D+7} S_4(y, x, d) - \frac{1}{90} \sum_{d=D-90}^{D-1} S_4(y, x, d), \quad (1)$$

where  $y, x$  represent the latitude and longitude of each pixel in the map, and  $d$  is the day. The resulting anomaly map shows maximum difference values of around  $\pm 0.06$  in the  $S_4$ .

Besides, the earthquakes occurring within the following 7 days, have been plotted in the same map to visually correlate if the pressure being built up in the lithosphere rocks before the earthquake occurs is actually impacting the ionosphere. The resulting anomaly map is shown in Fig. 1 for Jan 23, 2020.

Another data source used to correlate with earthquake events is the geomagnetic field and the plasma density data from ESA Swarm mission. Swarm constellation consists of 2 satellites, Alpha and Charlie, orbiting side-by-side at 460 km altitude and a third one, Bravo, at 530 km, all of them in polar orbits. Swarm performs high-precision and high-resolution measurements of the geomagnetic field strength and direction and plasma density at the orbital altitude.

### 3. RESULTS

The search of correlations between earthquakes and ionospheric activity has begun with the largest earthquakes in 2020. One of the cases studied was an earthquake happening in the Caribbean Sea, between Cuba and Jamaica on Jan 28, 2020, with a magnitude of 7.7 [6]. The hypocenter was located at 14.9 km depth undersea at around 123 km NNW from the coast of Jamaica at 19:10 UTC (14:10 LT). The contours of the intensity shake-map are shown in Fig. 2.

In the  $S_4$  anomaly map, an increase in the activity is observed starting around Jan 20 (8 days before the earthquake), then having a maximum on Jan 23 and 24 and continue decreasing during Jan 29 and 30, finally stabilizing around near-zero values. Four selected days are presented in Fig. 3. The perturbation size is approximately 500 km radius around the

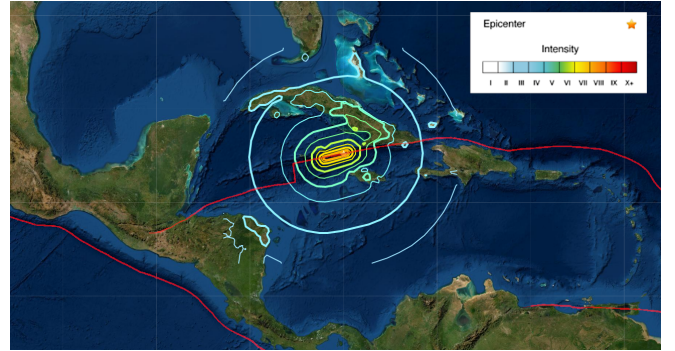


**Fig. 2:** Modified Mercalli Intensity (MMI) shake-map contours around the epicenter of the Caribbean earthquake on Jan 28, 2020 earthquake (magnitude 7.7), also showing the plate boundaries.

epicenter, similar to the shake-map contours’ size shown in Fig. 2.

To compare this anomaly in the  $S_4$  extracted from CYGNSS data, Fig. 4, shows two variables detected by ESA Swarm satellites Alpha (blue), Bravo (red) and Charlie (Green), during the months before and after the earthquake. The first one is the fluctuations in the plasma density ( $\Delta N_e 40s$ ). This parameter measures the difference between the actual electron density and the average value throughout 40 s, and it can detect perturbations in the order of 300 km and smaller. The second measurement presented is the residuals of the magnetic field intensity with respect to the geomagnetic model CHAOS-7 [7], and it is plotted as  $F_{res\_Model}$  in nT.

This data corresponds to a period from Jan 1 to Feb 29, 2020, in a rectangular region of 1800 x 1500 km around the epicenter of the Caribbean earthquake in Jan 28. In Fig. 4a, it is observed that the plasma density has larger peak fluctuations during January, in particular from Jan 3 to Jan 24, before the earthquake than in February.

In Fig. 4b, magnetic field intensity residuals are plotted, showing relatively homogeneous negative deviations from the magnetic model during the whole period in the two satellites with available data (Alpha and Bravo).

A second strong earthquake in 2020 happened in the coast of Mexico, in Oaxaca state, on Jun 23, 2020 [8], which inten-

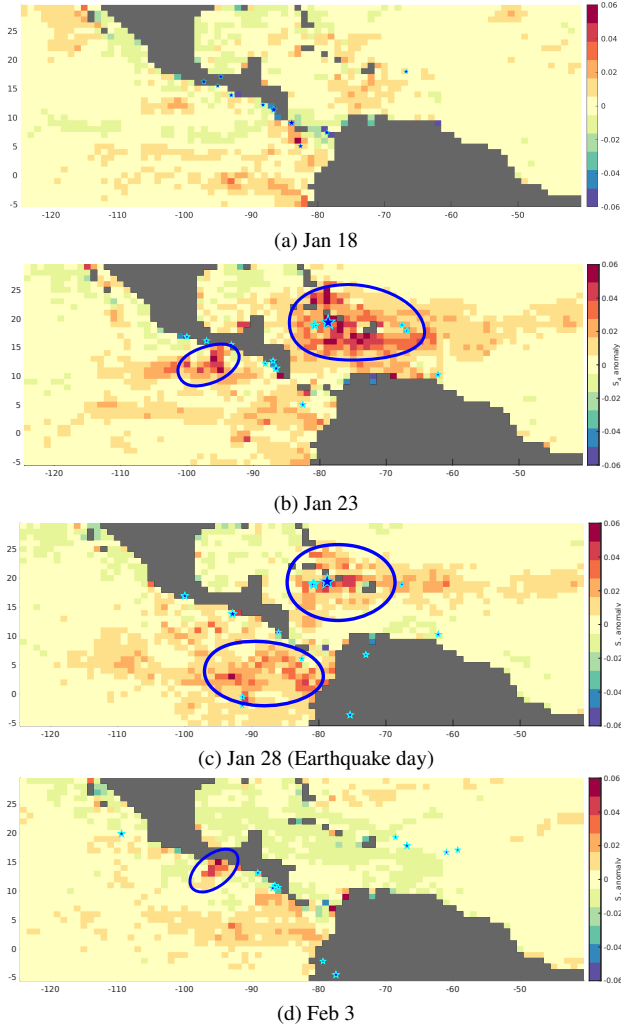


**Fig. 3:**  $S_4$  anomaly map for selected days around the Caribbean earthquake on Jan 28, with a resolution of  $1^\circ$  per pixel. Stars represent the earthquake's epicenters with magnitudes  $\geq 4.5$  in the next 7 days.

sity contour shake-map is shown in Fig. 5. It was a 7.4 magnitude earthquake in an underground point 20 km deep. The  $S_4$  anomalies map for selected days is shown in Fig. 6.

In Fig. 6b it can be seen a slightly circular peak in the  $S_4$  around the earthquake, in both Mexico shores, the Pacific one, close to the Earthquake epicenter, and the Gulf of Mexico one. This perturbation built up in the days following Jun 14 (Fig. 6a), and then disappeared by Jun 26 (Fig 6c).

#### 4. CONCLUSION

This work continues the study initiated in [4] using a novel technique to infer ionospheric parameters using GNSS-R data, with good availability in tropical and equatorial oceanic regions. This technique could be highly profitable for more

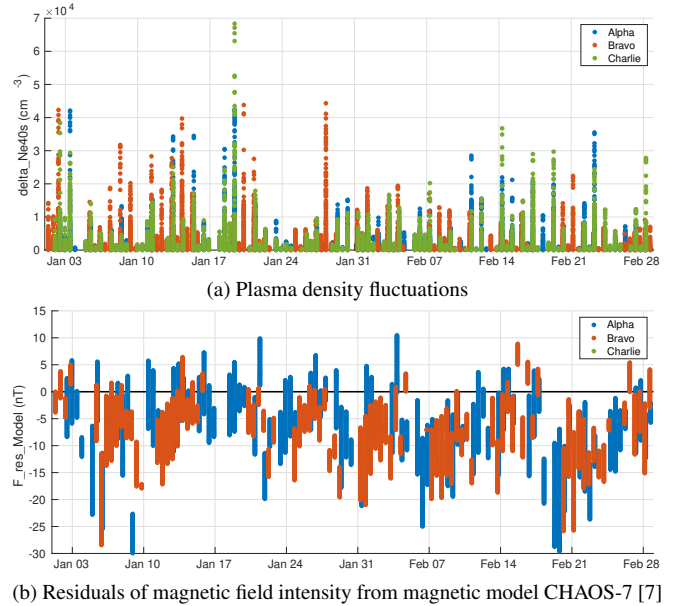


**Fig. 4:** Plasma density and geomagnetic measurements observed by Swarm during 2 months before and after the Jan 28 Caribbean earthquake within a region of  $1800 \times 1500$  km around the epicenter.

extensive, global ionospheric monitoring [5], as compared to ground-stations-based methods, in which only local activity may be detected.

Using this global indicator, patterns in the  $S_4$  behavior can be extracted to better monitor ionospheric activity produced by external Earth factors but also activity related with seismic events and earthquakes. With the availability of data over oceans, also undersea earthquakes can be studied, which constitute a large portion of the total number of earthquakes.

The work presented in this paper represents only a small fraction of the study that can be performed with this new way of monitoring the ionosphere. At the conference, correlations with other geophysical variables and other events will be presented. Future studies will incorporate as well other geomagnetic and solar parameters to discard possible false alarms.

It is significant to note that some of the events detected in the  $S_4$  anomalies map can be produced by other causes, like Equatorial Plasma Depletions or even large cyclones or hurricanes as some studies have shown [9], although it is not the case in the examples presented. Future studies will be conducted to find more indicators on this kind of ionospheric precursors for earthquake events.

#### 5. ACKNOWLEDGEMENTS

This work was supported by the Spanish Ministry of Science, Innovation and Universities and EFRD, "Sensing with Pioneering Opportunistic Techniques" SPOT, grant RTI2018-

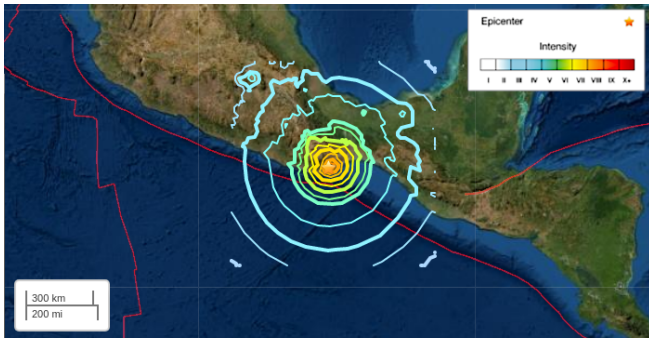


**Fig. 5:** MMI shake-map contours around the epicenter of the Oaxaca earthquake on Jun 23, 2020 earthquake (magnitude 7.4), also showing the plate boundaries.

099008-BC21/AEI/10.13039/501100011033, and by the Unidad de Excelencia Maria de Maeztu MDM-2016-0600.

## 6. REFERENCES

- [1] C. Tape, A. T. Ringler, and Don L. Hampton, “Recording the Aurora at Seismometers across Alaska,” *Seismological Research Letters*, vol. 91, no. 6, pp. 3039–3053, nov 2020.
- [2] A. T. Ringler, R. Anthony, D. Wilson, A. C. Claycomb, and J Spritzer, “Magnetic field variations in Alaska: Recording space weather events on seismic stations in Alaska,” *Bulletin of the Seismological Society of America*, vol. 110, no. 5, pp. 2530–2540, oct 2020.
- [3] L. Gheonjian, T. Paatashvili, and G. Kapanadze, “ELF radio emission associated with strong M6.0 earthquake,” in *2017 XXIIInd International Seminar/Workshop on Direct and Inverse Problems of Electromagnetic and Acoustic Wave Theory (DIPED)*, 2017, pp. 29–30.
- [4] A. Camps, H. Park, G. Foti, and C. Gommenginger, “Ionospheric effects in GNSS-Reflectometry from space,” *IEEE Journal of Selected Topics in Applied Earth Observations and Remote Sensing*, vol. 9, no. 12, pp. 5851–5861, 2016.
- [5] C. Molina and A. Camps, “First Evidences of Ionospheric Plasma Depletions Observations Using GNSS-R Data from CYGNSS,” *Remote Sensing*, vol. 12, no. 22, pp. 3782, nov 2020.
- [6] USGS, “M 7.7 - 123km NNW of Lucea, Jamaica,” <https://earthquake.usgs.gov/earthquakes/eventpage/us60007idc>, [Online; accessed 27-December-2020].
- [7] Christopher C. Finlay, Clemens Kloss, Nils Olsen, Magnus D. Hammer, Lars Tøffner-Clausen, Alexander

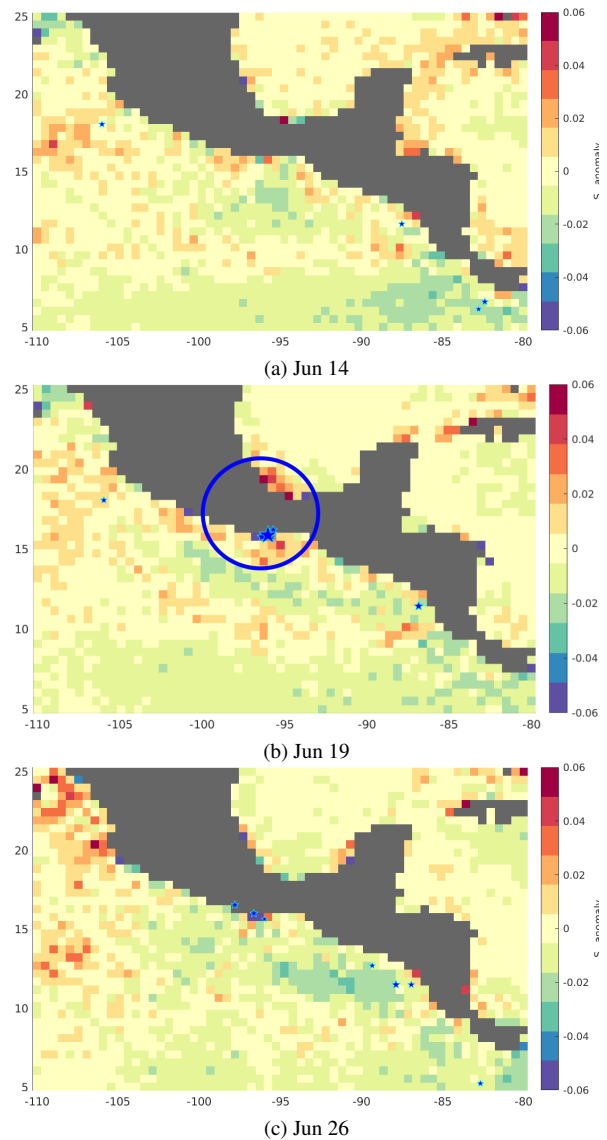


**Fig. 6:**  $S_4$  anomaly map for selected days around the Oaxaca earthquake on Jun 23, with a resolution of  $0.5^\circ$  per pixel.

Grayver, and Alexey Kuvshinov, “The CHAOS-7 geomagnetic field model and observed changes in the south atlantic anomaly,” *Earth, Planets and Space*, vol. 72, no. 1, Oct 2020.

- [8] USGS, “M 7.4 - 9 km SE of Santa María Xadani, Mexico,” <https://earthquake.usgs.gov/earthquakes/eventpage/us6000ah9t>, [Online; accessed 20-December-2020].
- [9] A. Camps, H. Park, J. M. Juan, J. Sanz, G. González-Casado, J. Barbosa, V. Fabbro, J. Lemorton, and R. Orús, “Ionospheric Scintillation Monitoring Using GNSS-R?,” in *IGARSS 2018 - 2018 IEEE International Geoscience and Remote Sensing Symposium*, 2018, pp. 3339–3342.